A novel infusion-drainage device to assess lower urinary tract function in neuro-imaging

Leitner, Lorenz ; Walter, Matthias ; Jarrahi, Behnaz ; Wanek, Johann ; Diefenbacher, Jörg ; Michels, Lars ; Liechti, Martina D ; Kollias, Spyros S ; Kessler, Thomas M ; Mehnert, Ulrich

DOI: https://doi.org/10.1111/bju.13655

A NOVEL INFUSION-DRAINAGE DEVICE TO ASSESS LOWER URINARY TRACT FUNCTION IN NEURO-IMAGING

Lorenz Leitner[1,2], Matthias Walter[1], Behnaz Jarrahi[3,4], Johann Wanek[1], Jörg Diefenbacher[5], Lars Michels[3], Martina D. Liechti[6], Spyros S. Kollias[3], Thomas M. Kessler[1] and Ulrich Mehnert[1]

1 Neuro-Urology, Spinal Cord Injury Center & Research, University of Zurich, Balgrist University Hospital, Zurich, Switzerland

2 Department of Urology, University Hospital Basel, Basel, Switzerland

3 Department of Neuroradiology, University Hospital Zürich, Zürich, Switzerland

4 UCLA Department of Psychiatry and Biobehavioral Sciences, Semel Institute for Neuroscience and Human Behavior, Los Angeles, CA, USA

5 Aroflex AG, Märstetten, Switzerland

6 Department of Brain Repair and Rehabilitation, Institute of Neurology, Unicersity College London, London, UK

BJU Int. 2017 Feb;119(2):305-316

PMID: 27617867

DOI: 10.1111/bju.13655

ABSTRACT

Objective: To evaluate the applicability and precision of a novel infusion-drainage device (IDD) for standardized filling paradigms in neuro-urology and functional magnetic resonance imaging (fMRI) studies of lower urinary tract (LUT) function/dysfunction.

Subjects/Patients and Methods: The IDD is based on electrohydrostatic actuation which was previously proven feasible in a prototype setup. The current design includes hydraulic cylinders and a motorized slider to provide force and motion. Methodological aspects have been assessed in a technical application laboratory as well as in healthy subjects (n=33) and patients with LUT dysfunction (n=3) undergoing fMRI during bladder stimulation. After catheterization, the bladder was pre-filled until a persistent desire to void was reported by each subject. The scan paradigm comprised automated, repetitive bladder filling and withdrawal of 100 mL body warm (37 °C) saline, interleaved with rest and sensation rating. Neuroimaging data were analysed using Statistical Parametric Mapping version 12 (SMP12).

Results: Volume delivery accuracy was between 99.1±1.2% and 99.9±0.2%, for different flow rates and volumes. Magnetic resonance (MR) compatibility was demonstrated by a small decrease in signal-to-noise ratio (SNR), i.e. 1.13% for anatomical and 0.54% for functional scans, and a decrease of 1.76% for time-variant SNR. Automated, repetitive bladder-filling elicited robust (P = 0.05, family-wise error corrected) brain activity in areas previously reported to be involved in supraspinal LUT control. There was a high synchronism between the LUT stimulation and the blood oxygenation level-dependent (BOLD) signal changes in such areas.

Conclusion: MR-synchronized IDD to routinely stimulate the LUT during fMRI in a standardized manner. The device provides LUT stimulation at high system accuracy resulting in significant supraspinal BOLD signal changes in interoceptive and LUT control areas in synchronicity to the applied stimuli. The IDD is commercially available, portable and multi-configurable. Such a device may help to improve precision and standardization of LUT tasks in neuro-imaging studies on supraspinal LUT control, and may therefore facilitate multisite studies and comparability between different LUT investigations in the future.

Keywords: lower urinary tract; functional magnetic resonance imaging (fMRI); visceral stimulation; interoception; bladder filling; magnetic resonance compatibility

INTRODUCTION

Over the last decades neuro-imaging studies have improved and expanded our knowledge of supraspinal lower urinary tract (LUT) function [1]. Earlier, pioneering studies used single-photon emission computed tomography [2] and positron emission tomography [3]. It was not until 2005 that functional magnetic resonance imaging (fMRI) was first used to examine supraspinal LUT control [4-6]. Since then, fMRI has emerged as the most popular approach in this field, as it can assess correlates of functional processes involved in LUT control in the human brain non-invasively, with a high spatial and acceptable temporal resolution [7]. Nevertheless, performing LUT stimulation tasks within a magnetic resonance (MR) environment is still a challenge, as the low signal-to-noise ratio (SNR) in echo-planar imaging (EPI) sequences as used in fMRI requires repeated captures of task-related data [8], i.e. repeated cycles of bladder filling and emptying [1]. Yet, most currently available devices that can be used for bladder filling are neither MR compatible, nor adapted to MR synchronization. Furthermore, they have only limited speed and accuracy of filling, and/or are not capable of also performing fluid withdrawal. Hence, recent fMRI studies used different approaches, i.e. manual and semiautomatic bladder filling protocols, to assess supraspinal network response to bladder filling and distention. Not surprisingly, the significance of supraspinal network activation and localization varies largely among studies [1, 9-11]; however, to analyse and interpret neuroimaging findings reliably based on visceral stimulation tasks, it is necessary to correlate task performance precisely with the neuroimaging signal acquisition [12].

To facilitate standardization and precision of task-related LUT neuroimaging studies we developed, based on our prototype [13], a commercially available, fully automated, flexibly programmable, MR-compatible and MR-synchronized infusion-drainage device (IDD).

SUBJECTS/PATIENTS AND METHODS

INFUSION-DRAINAGE DEVICE

The MR-compatible IDD is based on an electrohydrostatic actuation principle [13]. All components inside the MR scanner room are non-ferromagnetic and operated from the MR control room using a personal computer. A schematic overview of the arrangement of the IDD within the MR scanner facility is shown in **Figure 1**.

The key components of the IDD (**Figure 2**) consist of two polypropylene hydraulic cylinders (Typ 1108 DN40; PSK Ingenieurgesellschaft GmbH, Erfurt, Germany), i.e. a master cylinder with a stainless steel piston rod, a slave cylinder with a plastic piston rod, and a bipolar stepper motor controlling a linear slider with a moving platform (T-LSR 150 B; Zaber Technologies Inc., Vancouver, Canada). The cylinders are bidirectly coupled through a 10-m flexible polyurethane tubing with an outer diameter of 5 mm and a wall thickness of 1.5 mm (TFU0805B-2; SMC Corp., Tokyo, Japan). The system operates with distilled water. The piston rod of the master cylinder (**Figure 2C** and **D**) is fixed to the moving platform of the computer-controlled motorized linear slider system (travel range of 150 mm at a 0.5-µm resolution; speed range 0.00465 mm/s to 20 mm/s). Movement of the linear slider causes motion in

the master piston rod, and a fluid flow, and pressure change in the hydraulic actuator. As a result of the pressure changes, fluid transmits the energy through the tube causing a controllable bi-directional (positive or negative pressure) movement of the slave piston.

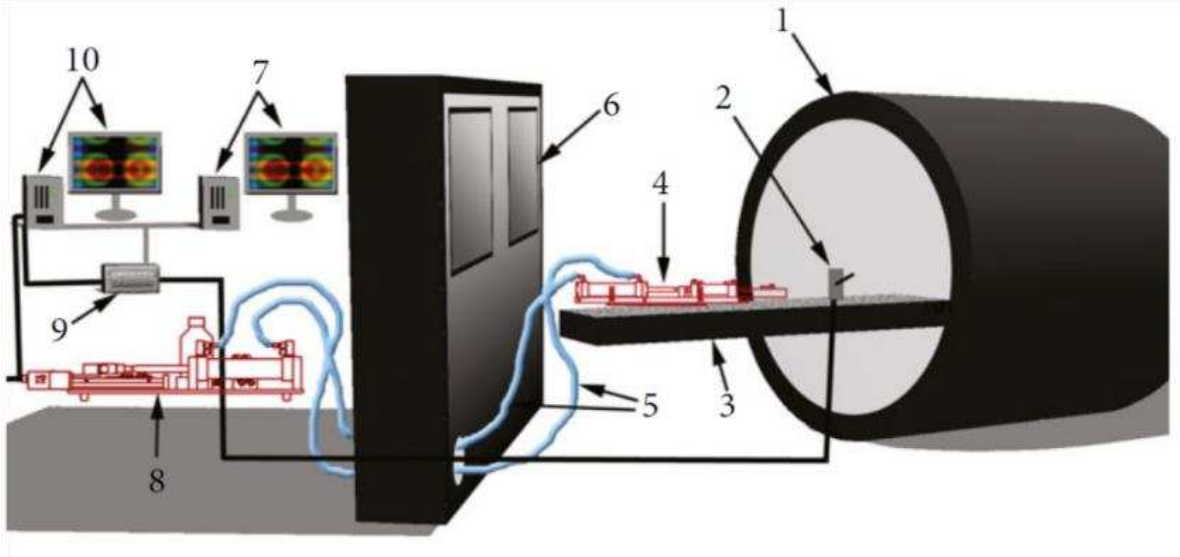

Figure 1 Schematic overview of the experimental setup and arrangement in the magnetic resonance (MR) facility. 1, MR scanner; 2, handheld response system (HRS); 3, moveable examination table; 4, slave cylinder assembly group, which connects the transurethral catheter with the bladder filling syringe and is placed between the legs of the subject/patient; 5, polyurethane tubing; 6, partition wall with electromagnetic shielding between MR scanner and MR control room; 7, MR control workstation; 8, master cylinder assembly group; 9, relay box with circuit board; 10, complementary PC to run the infusion-drainage device and HRS operational software. PC, personal computer.

The slave piston (**Figure 2E** and **F**) is connected to a commercially available, standard single-use 100-mL polypropylene syringe (Ominifix; B Braun Melsungen AG, Melsungen, Germany; movement of the syringe piston of 1 mm corresponds to 1 mL). The subject's bladder can be filled and drained through a single-use transurethral catheter attached to the syringe (**Figure 2E**).

To aerate the IDD and prevent a vacuum, a water-filled reservoir (**Figure 2C** and **D**) is integrated parallel to the cylinders and connected over check valves (AKH08A; SMC Corp., Tokyo, Japan). Pressure transducers (PAA-21 Y; Keller AG für Druckmesstechnik, Winterthur, Switzerland) allow a real-time tracing of the pressures in the IDD to monitor whether the system works appropriately or not.

Similarly to our prototype setup [13], we included a 12-bit multifunction USB data acquisition device (USB-6008; National Instruments, TX, USA) as an interface between the IDD and MRI scanner, and also to sample signals from the IDD. During fMRI, the data acquisition device also detects the transistor–transistor logic signals outputted by the MR scanner to synchronize the system with the image acquisition. Using the data acquisition device, multiple feedback devices, such as a fibre optic-based multi-configurable handheld response system (HRS) [14] to assess real-time sensory feedback (described later), or a transducer for measuring intravesical pressure, can be implemented.

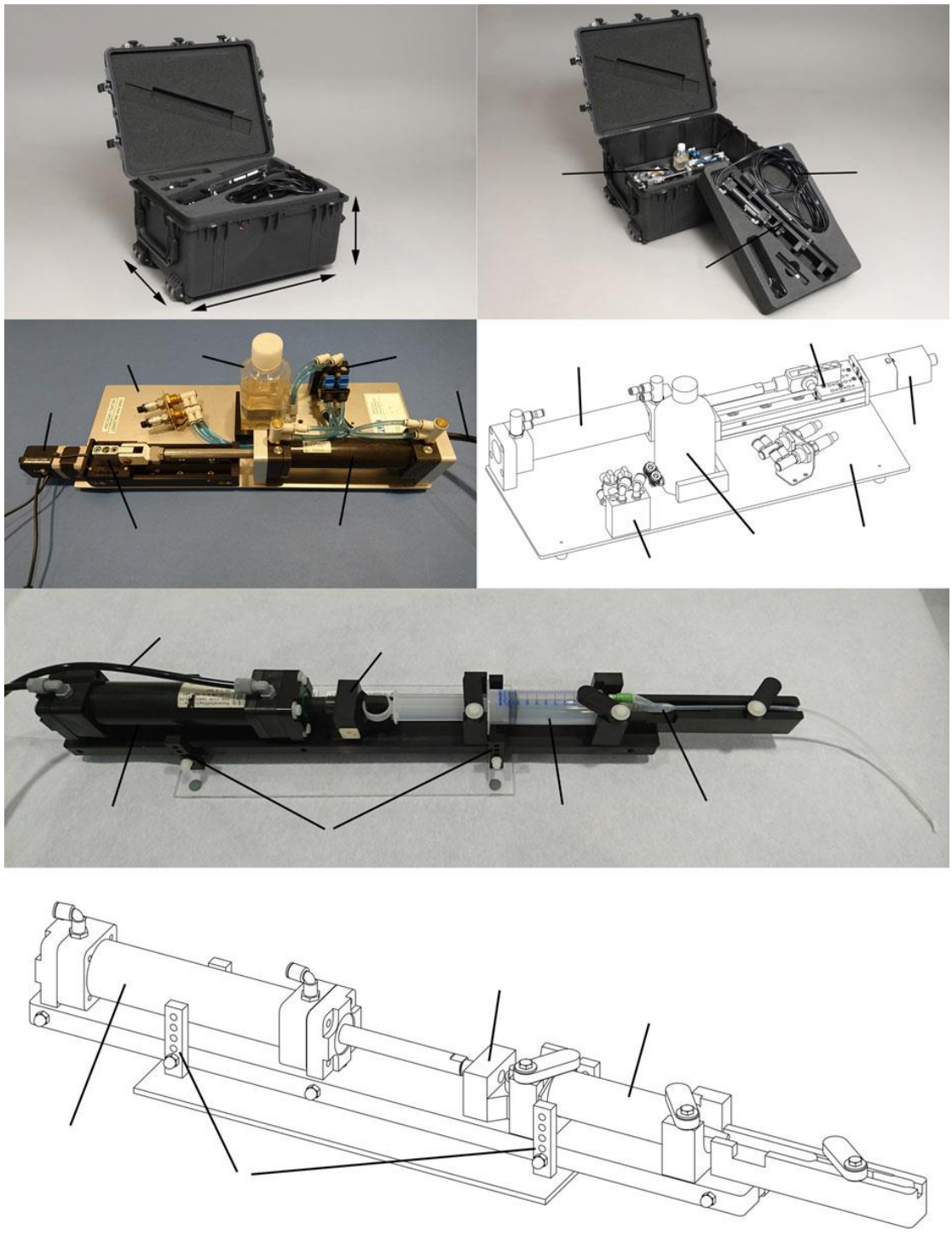

Figure 2 The transport case and technical components of the infusion-drainage device (IDD). For easy transportation and safe storage, the IDD can be placed into a wheeled hard-top case molded with foam x = 62 cm, y = 80 cm, z = 45 cm (A,B). The three main components of the IDD are the hydraulic master cylinder assembly group (C,D), a bipolar stepper motor driving the piston of the master cylinder (C), and a hydraulic slave cylinder assembly group (E,F). 1, master cylinder assembly group stored in the hard-top case; 2, polyurethane tubing (10 m) that connects the master and slave cylinders; 3, slave cylinder assembly group; 4, bipolar stepper motor (T-LSR 150 B, Zaber Technologies Inc., Vancouver, Canada); 5, linear slider with moving platform and fixation to the piston rod of the master cylinder; 6, base plate of the master cylinder assembly group; 7, water reservoir for fast and easy deairing; 8, hydraulic master cylinder made of polypropylene; 9, distribution board with check valves; 10, hydraulic slave cylinder made of polypropylene; 11, fixation rack of the slave cylinder with the possibility to adapt the height to the individual subject/patient; 12, slider, connecting the piston of the slave cylinder with the piston of the syringe containing the bladder filling fluid; 13, standard single-use 100-mL polypropylene syringe; 14, Foley catheter for transurethral placement.

OPERATIONAL SOFTWARE

The real-time custom-made operational control software for this device is based on C/C++ using Visual Studio 2008 (Microsoft, Redmond, WA, USA) [13]. The National Instruments LabView™ software package (National Instruments, TX, USA) as well as the built-in motion controller provided by Zaber Technologies (Vancouver, Canada) are implemented. The software offers an all-in-one control tool to operate the IDD and also additional devices, such as the HRS, to quantitatively measure responses to the stimulus/task generated by the IDD, e.g. degree of desire to void. Adjusting the stepper motor variables, flow rate, time and volume, as well as the numbers of repetitions, can be accomplished by the operational software. Synchronization with the MR scanner is achieved via the transistor–transistor logic signal outputted by the MR scanner at the onset of each EPI volume of functional series. Only the first transistor–transistor logic signal is used to start the computerized and temporal standardized stimulation paradigm. IDD and HRS data are stored in a separate log file.

INFUSION-DRAINAGE DEVICE PERFORMANCE TEST

To evaluate the performance quality of the IDD, volume delivery accuracy was tested at different flow rates, i.e. 80, 133, 200 and 400 mL/min, and different infusion times, i.e. 3, 7.5, 15, 30 and 45 s, using an Urocap IV scale (Laborie International, Ontario, Canada). According to the feasibility test in humans (eight blocks, infusion/withdrawal volume of 100 mL at a flow rate of 400 mL/min, see below), eight blocks of repetitive infusion and withdrawal cycles, using a 0.9% sodium chloride solution (Braun Melsungen AG, Melsungen, Germany; for the IDD performance test at room temperature, ~25 °C), were performed.

MRI

We evaluated MR compatibility using a Philips Ingenia 3 Tesla MRI system (Philips Medical Systems, Best, The Netherlands) at the University Hospital Zürich equipped with a standard 15-channel head coil array and a proton sphere phantom filled with 5 mL/L 98% acetate (CH3COOH), 10 mL/L 80% ethanol (CH3CH2OH), 8 mL/L 98% phosphorus acid (H3PO4), 1 mL/L 1% Arquad® solution, 120 mg/L anhydrous copper sulphate (CuSO4), and 380 mL of demineralized water. fMRI Images were acquired using an EPI T2*-sensitive sequence (echo time = 30 ms, repetition time = 2000 ms, flip angle = 80 °, field of view = 240 mm × 135mm × 240 mm, image matrix = 96 × 96, voxel size = 3 mm × 3 mm × 3 mm, number of slices 34). Further, we collected a high-resolution three-dimensional T1-weighted gradient echo sequence (echo time = 3.1 ms, repetition time 6.9 ms, flip angle = 8 °, field of view 256 mm × 256 mm × 180 mm, imaging matrix = 256 mm × 256 mm, voxel size = 1 mm × 1 mm × 1 mm, number of slices = 180). All images were obtained in an oblique axial orientation covering the entire brain, including the cerebellum and brainstem.

FEASIBILITY TEST IN HUMANS

Pilot tests were approved by the local ethics committee (Kantonale Ethikkommission Zürich, KEK-ZH-Nr. 2011- 0346) and registered at ClinicalTrials.gov (NCT01768910). We recruited 33 right-handed healthy subjects (16 females, 17 males) with unimpaired LUT function (**Table 1**) and no history of neurological disorder, and three patients with LUT dysfunction/symptoms (**Table 2**).

Table 1 Characteristics of healthy subjects.

Gender	Female (*n*=16)		Male (*n*=17)		*P**
Age	33±10		36±12		0.33
Prefilling volume, mL	444±115		469±149		0.59
Ratings		*P***		*P***	
Desire to void after infusion	8.38±0.97	0.00	7.45±1.61	0.00	0.53
Desire to void after drainage	5.31±1.32		3.93±1.49		0.01
Discomfort after infusion	0.9±0.73	0.03	1.23±1.56	0.05	0.44
Discomfort after drainage	0.56±0.32		0.54±0.31		0.84

*p-value for unpaired t-test to reveal difference in subjects' characteristics between gender. **p- value for paired t-test to reveal differences in ratings, i.e. urge and discomfort after infusion and drainage.

Table 2 Characteristics of patients.

Diagnosis Gender	NNOAB Female		MS Male		SCI AIS D sub TH11 Male	
Age	29		44		41	
Prefilling volume, mL	200		120		230	
Ratings		*P*		*P*		*P*
Desire to void after infusion	9±1.1	≤0.01	9.9±0.1	≤0.01	7.5±2.4	≤0.01
Desire to void after drainage	0.5±0.4		0.9±0.9		1±1.5	
Discomfort after infusion	8.2±1.4	≤0.01	9.2±1.2	≤0.01	3.9±1	0.41
Discomfort after drainage	0.4±0.4		1.1±0.5		3.5±1.3	

AIS, American Spinal Injury Association Impairment scale; MS, multiple sclerosis; NNOAB, non-neurogenic overactive bladder; SCI, spinal cord injury. P-value for paired t-test to reveal differences in ratings, i.e. urge and discomfort after infusion and drainage.

After written informed consent was obtained, subjects were placed in the scanner in a supine position. Thereafter, a soft 14-Fr silicon transurethral catheter (UROMED Kurt Drews GmbH, Oststeinbek, Germany) was introduced using a non-anaesthetic lubricant (Endosgel®, FARCO-PHARMA GmbH, Cologne, Germany).

To assess fluctuations in the subjective sensations throughout the entire LUT stimulation task, and therefore to evaluate the effect of fluid infusion and withdrawal by the IDD on the subject's sensory-perceptual level, a custom-designed MR-compatible HRS, described previously [14], was used.

SCAN PARADIGM

Before the EPI scans, the bladder was pre-filled with sterile body warm (37 °C) saline until subjects reported a persistent desire to void, i.e. six out of 10 on the visual analogue scale (VAS). Thereafter, eight blocks of repetitive infusion and withdrawal of 100 mL saline using the IDD were performed (**Figure 3).** A total of 450 functional scans were acquired. After an initial phase of 60 s REST (visual fixation) and two baseline RATINGS (rating of desire to void and discomfort on a projected VAS using the HRS, each 7 s), each block comprised the following conditions: INFUSION (automated bladder filling of 100 mL body warm (37 °C) saline, 15 s), PLATEAU (9 s), REST (visual fixation, 7–9 s), two RATINGS (2 × 7 s), WITHDRAWAL (automated bladder draining of 100 mL, 15 s), PLATEAU (15 s), two RATINGS (2 × 7 s), and another REST condition (visual fixation, 7–9 s) [15, 16]. The scan was finalized with a REST condition of 60 s.

During the RATING conditions subjects rated their desire to void (7 s) and discomfort (7 s) on a projected VAS (0–10) using the HRS.

During all other conditions, subjects were instructed to focus on a displayed fixation cross.

DATA ANALYSIS

Static SNR was evaluated for anatomical and functional images by a signal-background method, i.e. by dividing the mean signal intensity within the phantom over the standard deviation of the background-signal (defined by four smaller regions of interest outside the phantom) corrected with the Rayleigh distribution factor. The time-variant SNR (tSNR) was measured [17] to define the time course stability and degree of signal distortion during the scan under different conditions, i.e. phantom only, phantom with installed and working IDD and HRS, placed 40 cm away from the phantom.

fMRI data were analysed using SPM 12 (Wellcome Trust Centre for Neuroimaging, London, UK). The first five (dummy) scans were removed to allow for longitudinal magnetization equilibrium. The pre-processing consisted of realignment, normalization to the Montreal Neurological Institute (MNI) brain template, temporal filtering (128 s) and special smoothing (6 mm) [18, 19]. Each subject was analysed separately {first (within-subject)-level analysis} using a general linear model convolved with a canonical haemodynamic response function [19]. Head-motion variables (translation and rotation values) were included in the general linear model as regressor of no interest. The design matrix of the general linear model for the first-level analysis consisted of the following three events INFUSION,

WITHDRAWAL and REST (60 s), i.e. pre-filled bladder (60 s; **Figure 3**). The contrast images were then used for a second (between-subject) level analysis.

To assess the bladder network in healthy subjects, an anatomical mask was created according to the study by Griffith et al. [9] containing bilaterally the pons, periaqueductal grey (PAG), frontal and prefrontal cortex (covering the motor [Brodmann area {BA} 4] and supplementary motor/premotor cortex [BA 6], as well as the dorsolateral [BA 8, 9 and 46], ventrolateral [BA 44, 45, and 47], orbitofrontal/orbital [BA 47, and 11] and frontopolar [BA 10] subdivisions), cingulate cortex (subdivided in anterior [BA 24, 32, and 33] and posterior [BA 23, 29, 30 and 31]), insula, thalamus, putamen, hypothalamus and the cerebellum, using the WFU PickAtlas (http://fmri.wfubmc.edu/software/pickatlas). For areas that did not show significant activation in the *a priori*-defined mask, i.e. cerebellum, hypothalamus, pons and PAG, we additionally used a small volume correction, only including the specific brain region. Considering the limited literature according to alterations of the known bladder network in patients, only whole-brain analyses were performed in this subgroup.

Figure 3 Scan paradigm of the task-related functional MRI (fMRI). The fMRI task starts with a pre-filled bladder volume, i.e. the bladder will be filled with body warm (37 °C) saline until a persistent desire to void is present. The fMRI starts with a 'baseline' REST (60 s, no specific stimulus or task is performed), a 'baseline' RATING of desire to void and level of discomfort, a short REST jittered between 7 and 9 s in which blood oxygen level-dependent (BOLD) activation resulting from motor activity during the previous RATING will return to baseline to avoid contamination of the following condition and conclude with a 'last' REST (60 s, no specific stimulus or task is performed). The eight specific task-related blocks consist of: (1) automated INFUSION of 100 mL warm saline; (2) plateau phase (bladder distention after INFUSION is perceived); (3) RATING of desire to void and level of discomfort; (4) short REST jittered between 7 and 9 s in which BOLD activation resulting from motor activity during the previous RATING will return to baseline to avoid contamination of the following condition; (5) automated WITHDRAWAL of 100 mL; (6) plateau phase (bladder distention after WITHDRAWAL is perceived); (7) RATING of desire to void and level of pain; and (8) short REST jittered between 7 and 9 s, in which BOLD activation resulting from motor activity during the previous RATING will return to baseline to avoid contamination of the following condition. Reproduced from [Protocol for a prospective neuroimaging study investigating the supraspinal control of lower urinary tract function in healthy controls and patients with nonneurogenic lower urinary tract symptoms, Walter M. et al., BMJ Open 2014, copyright notice 07/2015] with permission from BMJ Publishing Group Ltd.

Data are presented as mean ± SD. Comparing unrelated samples, i.e. female vs male subjects, the unpaired *t*-test, for related samples, i.e. desire to void and level of discomfort (INFUSION vs WITHDRAWAL), the paired *t*-test was used, respectively. Statistical analyses were performed using Statistical Package for the Social Sciences (SPSS) V22 (IBM, Armonk, NY, USA). For the fMRI group results, a P value ≤0.05 (using the family-wise error [FWE] correction) [20] was considered statistically significant.

RESULTS

INFUSION-DRAINAGE DEVICE PERFORMANCE TEST

The results of the volume delivery accuracy of the IDD are shown in **Table 3**. Precision of the delivered volume over eight cycles of infusion and withdrawal was between 99.1±1.2% and 99.9±0.2%, for different flow rates and volumes. Time delay between the movement of the stepper motor and movement of the master as well as the slave piston rod, i.e. fluid transfer, was 1.31±0.21 s (**Fehler! Verweisquelle konnte nicht gefunden werden.**).

Table 3 Accuracy for volume delivery.

Set flow time at 15 s modulate flow rate			
Flow rate, mL/min	80	200	400
20	50	100	
Infusion Volume, mL	19.91±0.27	49.94±0.27	100.14±0.16
Infusion volume block 1, mL	20.49	49.81	100.08
Infusion volume block 8, mL	19.82	50.37	100.08
Withdrawal volume, mL	19.71±0.19	49.79±0.33	100.06±0.16
Withdrawal volume block 1, mL	19.66	49.78	100.25
Withdrawal volume block 8, mL	19.82	50.15	100.08
Overall volume transport accuracy*, %	99.1±1.2	99.7±0.6	99.9±0.2
Set flow rate at 400 mL/min modulate infusion/drainage time			
Flow time, s	3	7.5	15
Expected volume, mL	20	50	100
Infusion Volume, mL	20.03±0.29	50.03±0.34	100.14±0.16
Infusion volume block 1, mL	19.48	49.1	100.08
Infusion volume block 8, mL	20.14	50.46	100.08
Withdrawal volume, mL	20.08±0.14	49.9±0.33	100.06±0.16
Withdrawal volume block 1, mL	19.84	49.31	100.25
Withdrawal volume block 8, mL	20.14	49.89	100.08
Overall volume transport accuracy*, %	99.7±1.1	99.9±0.6	99.9±9.2
Set infusion/drainage volume at 100 mL modulate flow rate			
Flow rate, mL/min	133	200	400
Expected volume, mL	100	100	100
Infusion Volume, mL	99.86±0.32	100.18±0.35	100.14±0.16
Infusion volume block 1, mL	99.72	100.39	100.08
Infusion volume block 8, mL	100.32	100.99	100.08
Withdrawal volume, mL	99.74±0.42	100.08±0.43	100.06±0.16
Withdrawal volume block 1, mL	100.01	100.41	100.25
Withdrawal volume block 8, mL	100.27	100.16	100.08
Overall volume transport accuracy*, %	99.8±0.4	99.9±0.2	99.9±0.2

*Average volume transport accuracy over eight blocks infusion and withdrawal according to the expected volume.

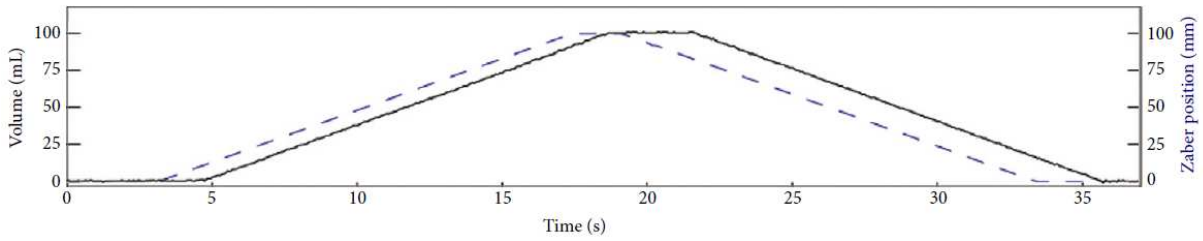

Figure 4 Sample infusion and drainage. Volume changes over time (straight black line) and position changes of the motorized linear slider (Zaber, blue dashed lines) over one cycle of infusion and drainage. The offset in the curves correspond to the time delay between movement of the linear slider and fluid transfer movement slave piston rod.

MR compatibility testing for the device with a phantom showed a decrease of overall SNR of 1.13% and 0.54% for anatomical and functional scans, respectively, and a tSNR of 1.76% for functional images (**Table 4**).

Table 4 MR compatibility tests with a phantom.

Test Condition	Anatomical SNR	Functional SNR	Functional tSNR
Baseline	741.04	783.64	271.95±31.46
Installed IDD HRS	749.54	787.86	276.82±31.59
Equivalence percentage	98.87	99.46	98.24

IDD, infusion-drainage device; HRS, handheld response system; SNR, signal-to-noise ratio; tSNR, time-variant SNR., Baseline = phantom only.

FEASIBILITY TEST IN HEALTHY SUBJECTS

Subject characteristics, including data on pre-filled bladder volume, desire to void and level of discomfort during bladder stimulation, are shown in **Table 1** and **Table 2**, respectively. In summary, over eight blocks, healthy subjects rated a significantly higher ($P \leq 0.05$) desire to void and level of discomfort for infusion versus drainage.

Using the *a priori*-defined regions of interest, healthy subjects showed significant activation ($P \leq 0.05$, FWE-corrected) in response to INFUSION vs REST in the bilateral frontal and prefrontal cortex, bilateral insula, bilateral thalamus, bilateral premotor cortex, left putamen and the cingulate cortex (detailed anatomical and spatial information: **Figure 5**, **Tables S1A–E**). Using a small volume correction for the bilateral cerebellum, bilateral hypothalamus, the PAG, and the pons, significant ($P \leq 0.05$, FWE-corrected) activation could also be shown in these areas.

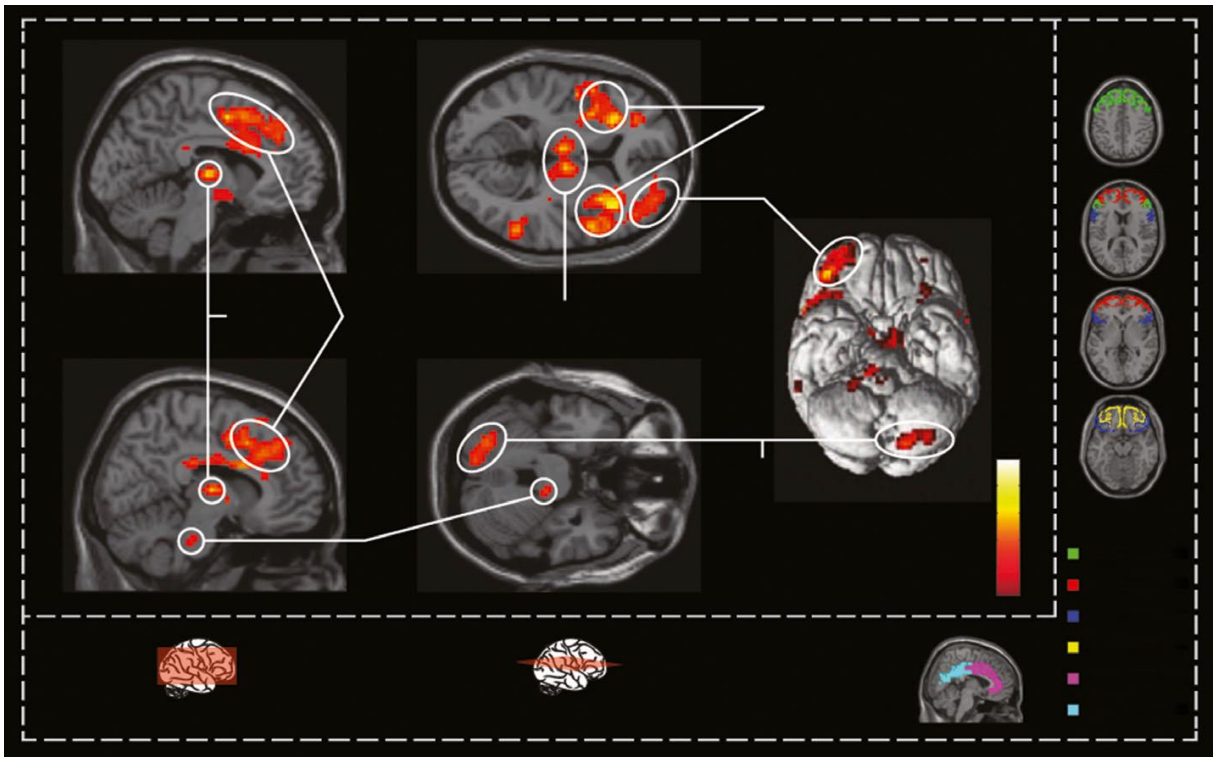

Figure 5 Second-level analysis of brain activity in response to automated, repetitive bladder filling (INFUSION) vs REST in 33 healthy subjects, using a predefined mask containing bilaterally the pons, periaqueductal grey (PAG), middle and inferior frontal gyrus, cingulate cortex, insula, thalamus, putamen, hypothalamus, premotor cortex, and the cerebellum. For display reasons, results are shown at a threshold of $P < 0.001$ uncorrected with cluster extend KE 42. The coordinates correspond to the brain template of the Montreal Neurological Institute and Hospital. The colour coding at the image frame indicates the further subdivisions of activated brain areas within the prefrontal (dorsolateral: Brodmann area [BA] 8, 9, 46; ventrolateral: BA 44, 45, 47; orbitofrontal/orbital: BA 47, 11; frontopolar: BA 10) and cingulate (anterior: BA 24, 32, 33; posterior: BA 23, 29, 30, 31) cortex. CC, cingulate cortex.

FEASIBILITY TEST IN PATIENTS

All patients rated a significantly higher ($P < 0.001$) desire to void for infusion vs drainage. Ratings for the level of discomfort were significantly higher (infusion vs drainage; $P < 0.001$), except for the patient with spinal cord injury.

Patients showed a heterogeneous pattern of significant activations ($P \leq 0.05$, FWE-corrected) in response to INFUSION vs REST in whole brain analyses (**Figure 6**). Activated brain areas included the bilateral frontal and prefrontal cortex, the cingulate cortex, the insula, the bilateral cerebellum and the somatosensory cortex, as well as the temporal and parietal lobe (**Tables S2A–C**). For both, healthy subjects and patients task-related adjusted BOLD signal response plotted over time showed changes in activation related to the different conditions of the scan paradigm (**Figure 7A–E**).

SAFETY

All subjects and patients tolerated the investigation well. An adverse event, as defined by the International Conference on Harmonisation Good Clinical Practice Guidelines (E6) [21] and International Organization for Standardization (ISO, 14155) [22], did not occur.

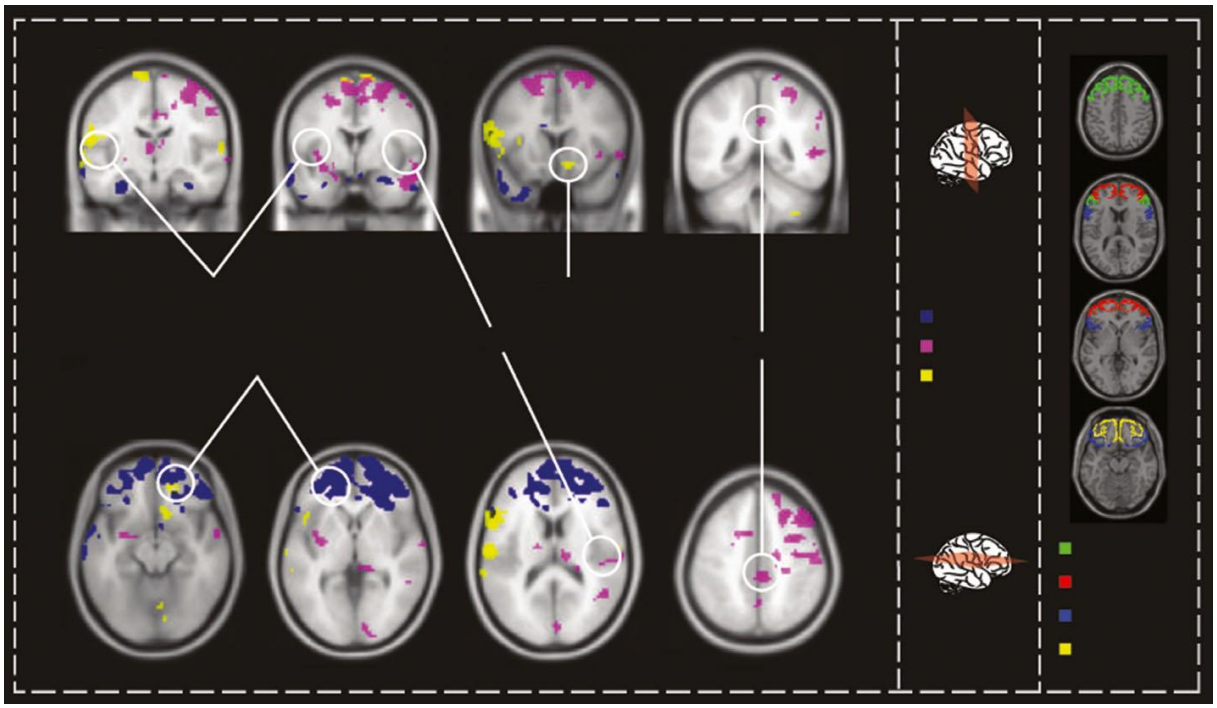

Figure 6 Overlaid brain activity (INFUSION vs REST) in patients with lower urinary tract dysfunction/symptoms. The activation pattern for the different patients are displayed in different colours; blue for the patient with non-neurogenic overactive bladder (NNOAB), pink for the patient with multiple sclerosis (MS) and yellow for the patient with spinal cord injury (SCI), respectively. For display reasons, results are shown at a threshold of $P < 0.001$ uncorrected. The coordinates correspond to the brain template of the Montreal Neurological Institute and Hospital. The colour coding at the image frame indicates the further subdivisions of activated brain areas within the prefrontal cortex (dorsolateral: Brodmann area [BA] 8, 9, 46; ventrolateral: BA 44, 45, 47; orbitofrontal/orbital: BA 47, 11; and frontopolar: BA 10).

DISCUSSION

MAIN FINDINGS

Our novel MR-compatible and MR-synchronized IDD, designed to stimulate the LUT during fMRI showed a consistent system performance with a high precision. Accuracy of the delivered volume was between 96.94 and 99.39%. All parts of the system within the MR scanner room are entirely non-ferromagnetic. Hence, MR compatibility could be proven by showing a low decrease in SNR and tSNR.

The feasibility test in humans showed robust supraspinal activation in areas related to LUT control. The BOLD signal increases in such areas were repeatedly related to the INFUSION and WITHDRAWAL conditions.

The real-time sensory feedback of healthy subjects and patients with LUT dysfunction correlated well with the IDD action, i.e. desire to void increased with infusion and decreased with fluid withdrawal. No adverse events occurred.

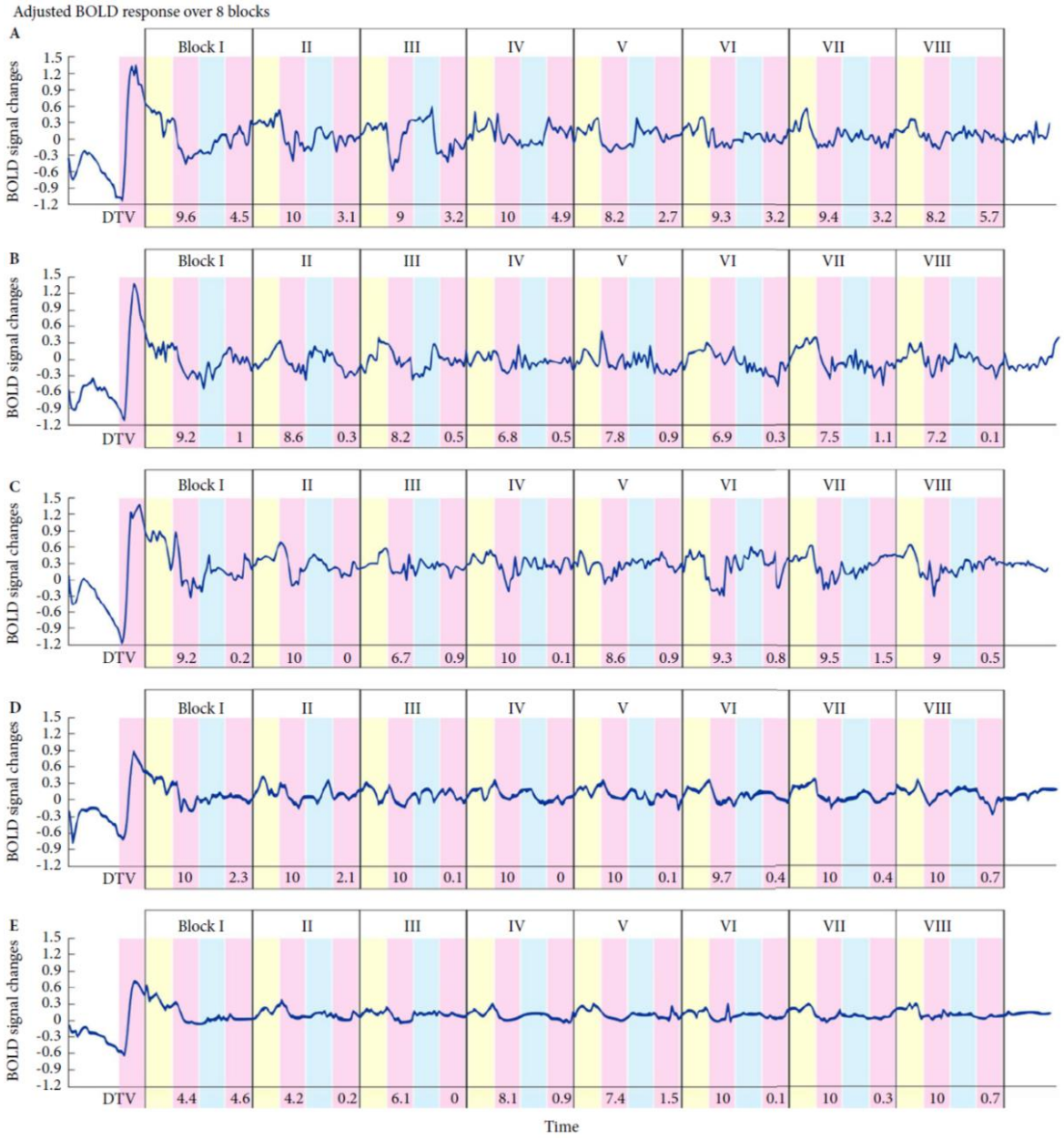

Figure 7 Adjusted blood oxygen level-dependent (BOLD) response over eight blocks in two healthy subjects (male and female) and patients, in the voxel with the global maximum response during INFUSION vs REST. The coordinates correspond to the brain template of the Montreal Neurological Institute and Hospital. (A) Healthy female subject (age 38 years, bladder pre-filling volume 300 mL): right middle frontal gyrus, x = 33, y = 53, z = -13. (B) Healthy male subject (age 37 years, bladder pre-filling volume 300 mL): right inferior frontal gyrus (triangle), x = 57, y = 32, z = 2. (C) Patients with nonneurogenic overactive bladder: right superior frontal medial gyrus, x = 12, y = 74, z = 1. (D) Patient with multiple sclerosis: right middle temporal gyrus, x = 54, y = - 49, z = 5. (E) Patient with spinal cord injury: left postcentral gyrus, x = -57, y = -19, z = 17. The colour backgrounds correspond to the different tasks, i.e. RATING/REST = pink, INFUSION/PLATEAU = yellow, WITHDRAWAL/PLATEAU = blue. Subjects rated desire to void (on a visual analogue scale from 0 to 10) after INFUSION and WITHDRAWAL are expressed in the RATING field. DTV, desire to void.

FINDINGS IN THE CONTEXT OF EXISTING EVIDENCE

The decisive aspect in every fMRI experiment is the study design [8]. The important aspect of precise timing and stimulation intensity for better interpretation of task-related supraspinal activity has been shown already [12]. It has been proven that automated computerized systems are superior in temporal precision and accuracy to conventional methods [23]; however, because of the strong magnetic field and the high radio frequency energy, the MR scanner room is a challenging environment in which to implement an automated computerized stimulation system [24]. Whenever a computerized stimulation system is used, subjects' safety, MR compatibility and high performance accuracy have to be guaranteed [23].

Various study designs were used to evoke brain responses through LUT stimulation. Kuhtz-Buschbeck et al. [5] and our own group [6, 25] applied periodic cycles of imagination of enhancing and suppressing the urge to void, contractions of the pelvic floor or manual filling of the bladder, to elicit supraspinal activity. Griffiths et al. [4] were the first to implement an adapted urodynamic method to examine supraspinal responses attributable to bladder distension. The resulting supraspinal activation in response to urodynamic filling demonstrated increased brain activation in the interoceptive circuit [26, 27]; however, BOLD signal responses and localization of BOLD signal changes in response to LUT stimulation tasks varied among studies, which might be, amongst other reasons, related to different scan protocols but also less accurate, non MR-synchronized task application. This latter aspect might be of specific relevance, considering that several studies on supraspinal LUT control could not provide significant results on a statistically corrected level, i.e. not using a correction for multiple comparisons [4, 10, 28]. An amelioration of significance levels using a standardized and tested device seems plausible and is supported by the significant multiple comparison corrected (FWE correction) findings in our group of 33 healthy subjects.

Although urodynamic devices are used in daily routine they may have limitations in the setting of MR neuroimaging. They must be placed outside the scanner room and can only be connected to a transurethral catheter through extension hoses. According to the manufacturer specification for a standard urodynamic system, the range of the infusion rate of the pump module is limited (5–140 mL/min, with an accuracy of ±5%). The pump module is not designed for fluid withdrawal. No reports are available as to whether the extension hose additionally impairs the working accuracy; however, precise volume delivery is questionable and accuracy has not been evaluated during fMRI. Using an MR-compatible syringe pump (e.g. HA2000WRMI; Harvard Apparatus, Massachusetts, USA; flow rate 0.0001 to 221 mL/min with an accuracy of ±0.5%) could overcome this problem. Nevertheless, the pre-determined operator software does not allow any synchronization with the MR scanner. Each stimulation has to be edited manually, making exact timing more difficult to achieve. Furthermore, such systems do not offer a solution by which additional data, e.g. behavioural data, could be implemented and recorded synchronously.

Based on our prototype [13], we developed a commercially available, MR-compatible and MR-synchronized IDD for routine use of bladder stimulation tasks in fMRI. The device provides a high accuracy in timing and filling volume with a continuously adaptable flow rate between 0.3 and 1200 mL/ min. Using the IDD, we showed that supraspinal areas of the LUT control network can be

significantly activated in a large sample of healthy subjects and also in an exemplary sample of patients. The temporal overlay of the adjusted BOLD signal increases demonstrated synchrony with the applied INFUSION and WITHDRAWAL conditions. In addition, the sensory responses of subjects and patients correlated well with the according IDD action, i.e. the desire to void was significantly higher and lower with INFUSION and WITHDRAWAL, respectively.

The current IDD version includes a fluid reservoir and a set of manual and check valves that enable a fast and complete evacuation of air (**Figure 2C–F**). In addition, the IDD is portable and easy to assemble, which enables convenient storage and use at multiple locations (**Figure 2A and B**). The whole system is available for ~$14,000, including a compact carrying case for safe transportation and a personal computer to run the system, which is reasonable compared with the costs for a conventional urodynamic system of $30,000–60,000. Furthermore, this device is expandable to allow additional measurements, e.g. implementation of pressure sensors to monitor intravesical pressure, suitable to be used in conjunction with other MR-synchronized devices, such as the HRS, and may be used for various applications including other organ systems such as the gastrointestinal tract, offering an all-in-one solution for MR synchronous measurements of visceral hollow organs.

LIMITATIONS

Currently, the IDD can only be used with a standardized 100 mL polypropylene syringe; however, it can be adjusted in order to operate with different volumes and syringes. The aim of this device is to cause filling or distention and subsequent deflation or emptying of visceral organs, such as the bladder. Hence, to investigate the central regulatory mechanisms during the initiation of micturition and actual micturition, such a device might not be useful.

CONCLUSION

For this novel MR-compatible and MR-synchronized IDD that has been designed to stimulate the LUT during fMRI we were able to show high accuracy in timing and infusion volume during automated, repetitive bladder filling in the MR scanner, eliciting significant activity in core areas of the supraspinal LUT control network.

This novel IDD has the potential to improve accuracy and standardization of neuroimaging protocols aiming to investigate supraspinal correlates of bladder filling and drainage. Using standardized protocols facilitates the reproducibility of study outcomes and comparison among studies.

ACKNOWLEDGMENTS

We would like to acknowledge the Swiss National Science Foundation (Grant No. 32003B_135774), Wings for Life, Emily Dorothy Lagemann Stiftung, and Swiss Continence Foundation (www.swisscontinencefoundation.ch) for financial support.

REFERENCES

1. Fowler CJ, Griffiths DJ. A decade of functional brain imaging applied to bladder control. Neurourol Urodyn. 2010;29(1):49-55.

2. Fukuyama H, Matsuzaki S, Ouchi Y, Yamauchi H, Nagahama Y, Kimura J, et al. Neural control of micturition in man examined with single photon emission computed tomography using 99mTc-HMPAO. Neuroreport. 1996;7(18):3009-12.

3. Blok BF, Willemsen AT, Holstege G. A PET study on brain control of micturition in humans. Brain. 1997;120 (Pt 1):111-21.

4. Griffiths D, Derbyshire S, Stenger A, Resnick N. Brain control of normal and overactive bladder. J Urol. 2005;174(5):1862-7.

5. Kuhtz-Buschbeck JP, van der Horst C, Pott C, Wolff S, Nabavi A, Jansen O, et al. Cortical representation of the urge to void: a functional magnetic resonance imaging study. J Urol. 2005;174(4 Pt 1):1477-81.

6. Zhang H, Reitz A, Kollias S, Summers P, Curt A, Schurch B. An fMRI study of the role of suprapontine brain structures in the voluntary voiding control induced by pelvic floor contraction. Neuroimage. 2005;24(1):174-80.

7. Ogawa S, Menon RS, Tank DW, Kim SG, Merkle H, Ellermann JM, et al. Functional brain mapping by blood oxygenation level-dependent contrast magnetic resonance imaging. A comparison of signal characteristics with a biophysical model. Biophys J. 1993;64(3):803-12.

8. Amaro E, Jr., Barker GJ. Study design in fMRI: basic principles. Brain Cogn. 2006;60(3):220-32.

9. Griffiths D, Tadic SD. Bladder control, urgency, and urge incontinence: evidence from functional brain imaging. Neurourol Urodyn. 2008;27(6):466-74.

10. Krhut J, Holy P, Tintera J, Zachoval R, Zvara P. Brain activity during bladder filling and pelvic floor muscle contractions: a study using functional magnetic resonance imaging and synchronous urodynamics. Int J Urol. 2014;21(2):169-74.

11. Mehnert U, Boy S, Svensson J, Michels L, Reitz A, Candia V, et al. Brain activation in response to bladder filling and simultaneous stimulation of the dorsal clitoral nerve--an fMRI study in healthy women. Neuroimage. 2008;41(3):682-9.

12. Buxton RB, Wong EC, Frank LR. Dynamics of blood flow and oxygenation changes during brain activation: the balloon model. Magn Reson Med. 1998;39(6):855-64.

13. Jarrahi B, Gassert R, Wanek J, Michels L, Mehnert U, Kollias SS. Design and Application of a New Automated Fluidic Visceral Stimulation Device for Human fMRI Studies of Interoception. IEEE J Transl Eng Health Med. 2016;4:2000108.

14. Jarrahi B, Wanek J, Mehnert U, Kollias S. An fMRI-compatible multi-configurable handheld response system using an intensity-modulated fiber-optic sensor. Conf Proc IEEE Eng Med Biol Soc. 2013;2013:6349-52.

15. Walter M, Michels L, Kollias S, van Kerrebroeck PE, Kessler TM, Mehnert U. Protocol for a prospective neuroimaging study investigating the supraspinal control of lower urinary tract function in healthy controls and patients with non-neurogenic lower urinary tract symptoms. BMJ Open. 2014;4(5):e004357.

16. Leitner L, Walter M, Freund P, Mehnert U, Michels L, Kollias S, et al. Protocol for a prospective magnetic resonance imaging study on supraspinal lower urinary tract control in healthy subjects and spinal cord injury patients undergoing intradetrusor onabotulinumtoxinA injections for treating neurogenic detrusor overactivity. BMC Urol. 2014;14:68.

17. Murphy K, Bodurka J, Bandettini PA. How long to scan? The relationship between fMRI temporal signal to noise ratio and necessary scan duration. Neuroimage. 2007;34(2):565-74.

18. Andersson JL, Hutton C, Ashburner J, Turner R, Friston K. Modeling geometric deformations in EPI time series. Neuroimage. 2001;13(5):903-19.

19. Friston KJ, Holmes AP, Poline JB, Grasby PJ, Williams SC, Frackowiak RS, et al. Analysis of fMRI time-series revisited. Neuroimage. 1995;2(1):45-53.

20. Hochberg Y, Benjamini Y. More powerful procedures for multiple significance testing. Stat Med. 1990;9(7):811-8.

21. International conference on harmonisation. Guideline for good clinical practice E6(R1). Current Step 4 version dated 10 June 1996. Access date June 2016. Available from: http://www.ich.org/fileadmin/Public_Web_Site/ICH_Products/Guidelines/Efficacy/E6/E6_R1_Guideline.pdf.

22. Clinical investigation of medical devices for human subjects – Good clinical practice. ISO 14155:2011. Access date June 2016. Available from: http://www.iso.org/iso/catalogue_detail?csnumber=45557.

23. Gassert R, Burdet E, Chinzei K. MRI-compatible robotics. Ieee Eng Med Biol. 2008;27(3):12-4.

24. Schaefers G. Testing MR safety and compatibility. Ieee Eng Med Biol. 2008;27(3):23-7.

25. Mehnert U, Michels L, Zempleni MZ, Schurch B, Kollias S. The Supraspinal Neural Correlate of Bladder Cold Sensation-An fMRI Study. Hum Brain Mapp. 2011;32(6):835-45.

26. Craig AD. How do you feel? Interoception: the sense of the physiological condition of the body. Nat Rev Neurosci. 2002;3(8):655-66.

27. Jarrahi B, Mantini D, Balsters JH, Michels L, Kessler TM, Mehnert U, et al. Differential functional brain network connectivity during visceral interoception as revealed by independent component analysis of fMRI time-series. Hum Brain Mapp. 2015;36(11):4438-68.

28. Griffiths DJ, Tadic SD, Schaefer W, Resnick NM. Cerebral control of the lower urinary tract: How age-related changes might predispose to urge incontinence. Neuroimage. 2009;47(3):981-6.

Abbreviations: BA, Brodmann area; BOLD, blood oxygenation level-dependent; EPI, echo-planar imaging; fMRI, functional MRI; FWE, family-wise error; HRS, handheld response system; IDD, infusion-drainage device; LUT, lower urinary tract; MR, magnetic resonance; PAG, periaqueductal grey; SNR, signal-to-noise ratio; tSNR, time-variant SNR.

SUPPLEMENTARY TABLES

Table 1 a-e: Healthy subjects (n=33): supraspinal areas with significant (p<0.05, FWE-2 corrected) task-related (INFUSION vs. REST) BOLD signal intensity increase.

a) Using a predefined anatomical mask containing the whole pons, periaqueductal grey (PAG), frontal cortex, cingulate cortex, insula, thalamus, putamen, hypothalamus, premotor cortex and the cerebellum, in each case bilateral.

Peak level *p* (FWE-corr.)	T score	MNI Coordinates [mm] x	y	z	Supraspinal region / area
0.000	8.57	54	5	19	Inferior frontal cortex (Operculum, BA 44) R
0.000	7.69	39	23	7	Inferior frontal cortex (Triangle, BA 45) R
0.005	6.32	33	14	10	Insula R
0.024	5.65	36	2	13	Insula L
0.000	7.23	-27	-1	13	Putamen L
0.018	5.78	-36	8	1	Insula L
0.001	7.00	33	41	28	Middle frontal cortex (BA 46) R
0.027	5.59	33	41	40	Middle frontal cortex (BA 46) R
0.002	6.71	-30	26	4	Insula L
0.008	6.14	-6	-16	4	Thalamus L
0.011	6.00	9	-13	7	Thalamus R
0.013	5.91	54	8	7	Inferior frontal cortex (Operculum, BA44) R
0.014	5.87	3	14	58	Supplementary motor area (BA 6) R
0.016	5.82	-3	14	49	Supplementary motor area (BA 6) L
0.018	5.76	-33	38	13	Inferior frontal cortex (Triangle, BA 45) L
0.020	5.73	6	11	25	Anterior cingulate cortex (BA 33) R
0.024	5.64	48	14	1	Inferior frontal cortex (Operculum, BA 44) R
0.034	5.50	9	14	43	Middle cingulate cortex (BA 24) R
0.035	5.49	39	8	55	Middle frontal cortex (BA 46) R
0.040	5.42	6	32	34	Middle cingulate cortex (BA 24) R
0.041	5.42	-48	-4	7	Rolandic operculum L
0.044	5.39	39	29	37	Middle frontal cortex (BA 46) R
0.049	5.34	-9	11	37	Middle cingulate cortex (BA 24) L

b) Using a small volume correction only including the cerebellum

Peak level *p* (FWE-corr.)	T score	MNI Coordinates [mm] x	y	z	Supraspinal region / area
0.026	4.93	-24	-73	-29	Cerebellum Crus I L
0.035	4.80	-12	-82	-29	Cerebellum Crus I L
0.039	4.76	30	-61	-50	Cerebellum R
0.041	4.73	-30	-76	-44	Cerebellum Crus II L

c) Using a small volume correction only including the hypothalamus

Peak level *p* (FWE-corr.)	T score	MNI Coordinates [mm] x	y	z	Supraspinal region / area
0.003	3.88	-9	-7	-8	Hypothalamus L/Thalamus L
0.004	3.74	-3	-1	-14	Hypothalamus L/Caudate L
0.004	3.54	3	-7	-11	Hypothalamus R/Thalamus R

d) Using a small volume correction only including the Periaqueductal gray

Peak level *p* (FWE-corr.)	T score	MNI Coordinates [mm] x	y	z	Supraspinal region / area
0.023	4.02	6	-16	-20	PAG/Para-Hyppocampus R

e) Using a small volume correction only including the pons					
Peak level		MNI Coordinates [mm]			Supraspinal region / area
p (FWE-corr.)	T score	x	y	z	
0.006	4.66	12	-28	-32	Pons R/Cerebellum R
0.017	4.23	212	-37	-35	Pons R/Cerebellum R
0.030	3.98	3	-34	-41	Pons R/Vermis

Table 2: Patients: Brain areas with significant (p<0.05, FWE-corrected) task-related (INFUSION vs. REST) signal intensity increase, whole brain analysis.

a) NNOAB patient: Female, age 29, bladder prefilling volume 200 mL					
Peak level		MNI Coordinates [mm]			Supraspinal region / area
p (FWE-corr.)	T score	x	y	z	
0.000	10.564	12	74	1	Superior frontal cortex med. (BA 10)R
0.000	10.128	42	44	1	Middle frontal cortex (BA 45/46) R
0.000	9.514	15	62	10	Anterior cingulate cortex (BA 32) R
0.000	8.885	-42	26	-23	Orbitofrontal cortex post. (BA 11) L
0.000	7.697	-54	14	-20	Superior temporal cortex (Temporal pole, BA 38) L
0.000	6.083	-51	2	-38	Inferior temporal cortex L
0.000	7.884	-30	17	-38	Middle temporal cortex (Temporal pole) L
0.000	7.112	-24	50	22	Superior frontal cortex (BA 10) L
0.000	7.106	24	14	-35	Superior temporal cortex (Temporal pole) R
0.000	6.749	30	26	4	Insula R
0.025	4.894	21	32	-5	Orbitofrontal cortex ant. (BA 12) R
0.000	6.505	21	32	-14	Orbitofrontal cortex ant. (BA 12) R
0.000	6.495	30	-4	-23	Hippocampus R
0.000	6.470	-27	59	28	Superior frontal cortex (BA 10) L
0.000	6.308	-51	35	-5	Inferior frontal cortex (Orbital, BA 45) L
0.001	5.592	-36	47	1	Middle frontal cortex (BA 46) L
0.003	5.391	-45	41	-17	Orbitofrontal cortex ant. (BA 47) L
0.000	6.197	54	8	-26	Middle temporal cortex (Temporal pole) R
0.000	5.928	3	35	-5	Anterior cingulate cortex (BA 24) R
0.000	5.912	39	53	-14	Orbitofrontal cortex ant. (BA 47)R
0.000	5.873	-57	-7	-8	Middle temporal cortex L
0.001	5.613	-6	26	13	Anterior cingulate cortex (BA 33) L
0.019	4.961	-12	20	22	Middle cingulate cortex (BA 24) L
0.001	5.546	-33	-7	-29	Fusiform gyrus L
0.019	4.961	-39	-7	-38	Inferior temporal cortex L
0.001	5.529	-12	20	-17	Gyrus rectus L
0.001	5.528	-60	5	-11	Superior temporal cortex L
0.002	5.472	36	17	-2	Insula R
0.003	5.368	-66	-7	-32	Inferior temporal cortex L
0.004	5.321	18	11	-8	Putamen R
0.004	5.312	-6	65	34	Superior frontal cortex (BA 9) L
0.004	5.289	6	5	-14	Caudate R
0.005	5.270	-60	20	7	Inferior frontal cortex (Triangle, BA 45) L
0.006	5.218	-39	38	13	Inferior frontal cortex (Triangle, BA 45) L
0.025	4.894	-27	38	13	Middle frontal cortex (BA 46) L
0.007	5.180	48	23	40	Middle frontal cortex (BA 46) R
0.008	5.161	-45	26	-14	Orbitofrontal cortex lat. (BA 45) L
0.008	5.151	-45	17	4	Inferior frontal cortex (Triangle, BA 45) L
0.011	5.091	-54	-46	4	Middle temporal cortex L
0.019	4.953	-57	-43	-5	Middle temporal cortex L

0.011	5.082	-66	-4	-11	Middle temporal cortex L
0.013	5.054	63	-16	-5	Superior temporal cortex R
0.014	5.028	-42	41	22	Middle frontal cortex (BA 46) L
0.015	5.015	21	5	-38	Middle temporal cortex (Temporal pole) R
0.016	4.994	45	-43	-29	Fusiform gyrus R
0.017	4.987	-42	11	-44	Inferior temporal cortex L
0.018	4.973	60	-10	-8	Superior temporal cortex R
0.020	4.946	-12	14	-11	Caudate L
0.030	4.852	12	44	-2	Middle frontal cortex (Orbital) R
0.031	4.843	27	-31	-26	Cerebellum R
0.031	4.837	0	53	34	Superior frontal cortex med. (BA 9) L
0.033	4.822	-66	-16	-14	Middle temporal cortex L
0.041	4.774	-24	47	31	Middle frontal cortex (BA 46) L
0.050	4.723	36	-4	-44	Fusiform gyrus R

b) MS patient: Male, age 44, bladder prefilling volume 120 mL

Peak level		MNI Coordinates [mm]			Supraspinal region / area
p (FWE-corr.)	T score	x	y	z	
0.000	5.872	54	-49	5	Middle temporal cortex R
0.001	5.743	-21	-91	-34	Cerebellum Crus II L
0.001	5.679	-6	-73	50	Precuneus L
0.001	5.639	9	53	-7	Middle frontal cortex (Orbital, BA 10) R
0.001	5.579	9	-73	53	Precuneus R
0.002	5.496	-30	-70	59	Superior parietal cortex L
0.003	5.462	0	-29	39	Middle cingulate cortex (BA 31) L
0.012	5.174	33	-79	-28	Cerebellum Crus I R
0.023	5.043	-24	-73	56	Superior parietal cortex L
0.032	4.976	-21	-43	74	Postcentral gyrus L
0.043	4.914	-3	62	-19	Medial orbitofrontal cortex (BA 11) L
0.049	4.887	21	-85	47	Superior occipital cortex R

c) SCI Patient: Male, age 41, bladder prefilling volume 230 mL

Peak level		MNI Coordinates [mm]			Supraspinal region / area
p (FWE-corr.)	T score	x	y	z	
0.001	5.626	-57	-19	17	Postcentral gyrus L
0.002	5.572	-48	20	14	Inferior frontal cortex (Triangle, BA45) L
0.002	5.569	-33	32	-13	Inferior frontal cortex (Orbital, BA 46) L
0.002	5.553	-12	-22	80	Paracentral lobule L
0.003	5.465	24	38	-16	Orbitofrontal cortex ant. (BA 12) R
0.005	5.341	63	-28	26	Rolandic operculum R
0.031	4.993	57	-34	26	Superior temporal cortex R
0.007	5.284	-9	47	-13	Middle frontal cortex (Orbital, BA 10) L
0.036	4.962	-54	5	26	Precentral gyrus L
0.044	4.919	30	41	26	Middle frontal cortex (BA 46) R
0.045	4.912	21	56	-7	Superior frontal cortex (BA 8) R

BA = Brodmann Area, , FWE = family-wise error, L = left cerebral hemisphere MNI = 12 Montreal Neurological Institute, MS = Multiple sclerosis, NNOAB = non-neurogenic 13 overactive bladder, R = right cerebral hemisphere, SCI = Spinal cord injury.